Absorption cross sections and number densities of electron and hole polarons in congruently melting $LiNbO_3$

2009 J. Phys.: Condens. Matter 21 015906

(http://iopscience.iop.org/0953-8984/21/1/015906)

J. Phys.: Condens. Matter **21** (2009) 015906 (6pp) doi:10.1088/0953-8984/21/1/015906

Absorption cross sections and number densities of electron and hole polarons in congruently melting $LiNbO_3$

C Merschjann[1], B Schoke[1], D Conradi[1], M Imlau[1], G Corradi[2] and K Polgár[2]

[1] Universität Osnabrück, Fachbereich Physik, D-49069 Osnabrück, Germany
[2] Research Institute for Solid State Physics and Optics, Hungarian Academy of Sciences, Budapest, POB 49, H-1525, Hungary

E-mail: cmerschj@physik.uni-osnabrueck.de

Received 25 April 2008, in final form 17 November 2008
Published 8 December 2008
Online at stacks.iop.org/JPhysCM/21/015906

Abstract
The number densities and absorption cross sections of both optically generated and reduction-induced small electron and hole polarons in $LiNbO_3$ are determined by means of time-resolved pump–multiprobe spectroscopy. The data are obtained for free (Nb_{Nb}^{4+}) and bound (Nb_{Li}^{4+}) electron polarons, bound Nb_{Li}^{4+}:Nb_{Nb}^{4+} electron bipolarons, and bound O^- hole polarons. The peak absorption cross sections are in the range of $\sigma_{pol} \approx (4\text{–}14) \times 10^{-22}$ m^2, comparable to that for Fe^{2+}. In all cases the ratio of occupied to unoccupied polaronic sites is less than 10^{-2}.

1. Introduction

The optical absorption properties of small polarons are of great interest in the field of photorefractive and nonlinear optics. Light-induced absorption (the photochromic effect) caused by optically generated small polarons is an important issue which strongly affects the performance of laser systems and which may result in catastrophic damage of nonlinear optical devices [1]. Among the materials showing polaronic photochromic effects are LiB_3O_5 [2], $KTiOPO_4$ [3], $LiTaO_3$ [4], $KNbO_3$ [5], and $LiNbO_3$ [6]. Due to its intrinsic defect structure, lithium niobate ($LiNbO_3$) turns out to be an ideal material for investigations of both optically generated and reduction-induced small polarons. At least three different kinds of small electron polarons have been identified so far: so-called free polarons (Nb_{Nb}^{4+}, FP; lower indices indicate substitution sites) [7], bound polarons (Nb_{Li}^{4+}, GP) [8], and bound bipolarons (Nb_{Li}^{4+}:Nb_{Nb}^{4+}, BP) [9]. The bound polarons are localized at Nb_{Li} antisite defects, occurring in congruently melting $LiNbO_3$ in a concentration of $[Nb_{Li}] \approx 1\%$ [10], while free polarons appear at regular Nb sites. Besides electron polarons, bound hole polarons (O^-, HP) are also found in the vicinity of Li vacancies V_{Li} [11–13]. All of these polarons are accompanied by strong, broad absorption bands in the blue–green (HP, BP, $\lambda = 500$ nm [9, 11, 13]), red (GP, $\lambda = 760$ nm [8, 14]), and near-infrared spectral range (FP, $\lambda = 1250$ nm [7]). While the single polarons (FP, GP, HP) are usually found as metastable states upon optical excitation with intense visible light [11, 12, 15–17], stable Nb_{Li}^{4+}:Nb_{Nb}^{4+} bipolarons can be created by thermal or electrochemical reduction [9, 15, 18, 19]. Only recently we reported on the influence of chemical reduction on the amplitudes of light-induced absorption changes [20, 21]. This effect was assigned to the simultaneous optical generation of single small polarons (FP, GP, HP) and optical dissociation of bipolarons. Thus, the number densities of optically generated small polarons crucially depend on the state of reduction [20].

In order to adequately investigate the properties of polarons in oxide materials, including charge transport and relations to extrinsic defect centers like $Fe^{2+/3+}$, a precise knowledge of the number densities of the various polarons created in the samples is desirable. However, up to now values could only be given for the absorption cross section of Nb_{Li}^{4+} in $LiNbO_3$ [14, 22, 23]. Data for the other polarons known to exist in lithium niobate are still missing—let alone the other oxide materials mentioned above.

In this work we show for the first time the possibility of *quantitatively* determining number densities and absorption cross sections of all four kinds of small polarons found in congruently melting $LiNbO_3$ by means of pump–multiprobe spectroscopy.

Table 1. List of the $LiNbO_3$ samples used for the investigations. All samples are grown from a congruent melt composition. Also given are the amplitudes of the transient light-induced absorption, α_{li}^{max}, for the different probe wavelengths. The values are taken from [20, 24, 25]. Cells marked '—' denote values not used in the present work.

				$\alpha_{li}^{max}(\lambda)$ (m^{-1})				
Sample	Dopant (mol%)	Reduced	Polaron types	488 nm	785 nm	1310 nm	I_p(GW m^{-2})	Ref.
cln0_2	—	No	GP, HP	21	30	—	760	[20]
cln800_1	—	Yes	GP, BP	−400	790	—	670	[20]
cln149912.1	MgO (4.2)	No	GP, HP	100	90	—	1400	[24]
cln140704.1	MgO (6.5)	No	FP, HP	150	—	165	1400	[25, 24]

2. Experimental details; principles of calculation

x-cut samples of congruently melting nominally pure $LiNbO_3$ (Crystal Technology, Inc.) and $LiNbO_3$:Mg (grown by K Polgár, [Mg] below (4.2 mol%) and above (6.5 mol%) the optical damage resistance threshold (ODRT)) were polished to optical quality. The thickness of the specimens was about 2 mm, and the total Fe impurity concentration did not exceed 5 ppm [20, 24]. In order to create stable bipolarons, one of the undoped samples was thermally reduced in vacuum ($p < 10^{-4}$ mbar) for 6 h at 1070 K. It is known that $LiNbO_3$ doped with MgO above the ODRT is free of antisite defects, so neither GP nor BP may occur. This was verified by reducing one specimen of $LiNbO_3$:Mg (6.5 mol%), which revealed solely the characteristic FP absorption band [7].

Thus, all four kinds of small polarons can be investigated by means of combined measurements for as-grown and reduced nominally pure and Mg-doped $LiNbO_3$ samples. A list of the specimens containing information about the treatment and the observable kinds of small polarons is given in table 1.

Measurements of the transient light-induced absorption $\alpha_{li}(t)$ were performed using a setup for time-resolved pump–multiprobe spectroscopy, described in [19, 20]. Here, intensities of the pump light $I_p \leqslant 760$ GW m^{-2} (undoped $LiNbO_3$) and $I_p \leqslant 1400$ GW m^{-2} ($LiNbO_3$:Mg) at a wavelength of $\lambda = 532$ nm were used. The wavelengths of the ordinary polarized probe light were chosen close to the respective maxima of the absorption bands of the polarons involved, i.e., $\lambda = 488$ nm (HP, BP), $\lambda = 785$ nm (GP), and $\lambda = 1310$ nm (FP). The calculations conducted here are based on the values for the amplitude of the transient light-induced absorption, α_{li}^{max}, given in table 1, which have been obtained using pump–multiprobe spectroscopy [20, 24, 25]. For an easier understanding, the relevant experimental spectra are additionally given in figures 1 and 2.

In order to calculate number densities and absorption cross sections we use the fundamental relation

$$\alpha_{li}(\lambda) = \sum_i \alpha_{li,i}(\lambda), \tag{1}$$

with

$$\alpha_{li,i}(\lambda) = N_{li,i}\sigma_i(\lambda), \tag{2}$$

where $N_{li,i}$ and $\sigma_i(\lambda)$ denote the light-induced number densities and absorption cross sections for the different kinds of polarons i. Note that $N_{li,i}$ is negative for optically dissociated species [20].

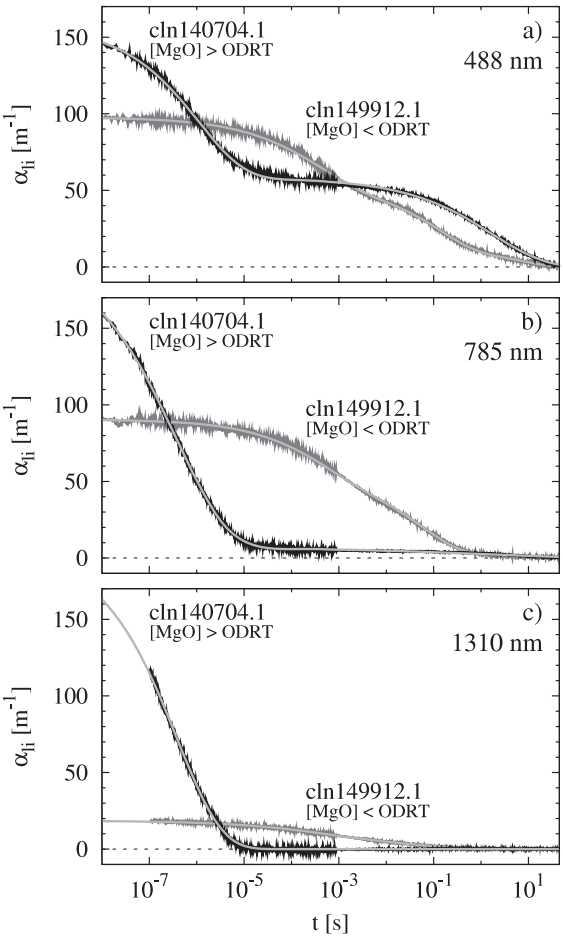

Figure 1. Development of the light-induced absorption in $LiNbO_3$:Mg below and above the ODRT for the three probe wavelengths at room temperature. The pump intensity is $I_p = 1400$ GW m^{-2}. For details see [24].

In the past, several attempts have been made to describe theoretically the spectral shape of the absorption bands of small polarons (see, e.g., [26–29] and figure 3, where the theoretical band shape for σ_{GP}, according to [26, 27], has been drawn as a dotted line). However, as seen in figure 3, for photon energies above the band maximum the absorption coefficient is substantially underestimated by the existing theories, yielding basically symmetric lineshapes [13]. It should be noted that the asymmetry of the lineshapes derived from the measured spectra is an effect by far outside the experimental error. This observation is not restricted to small

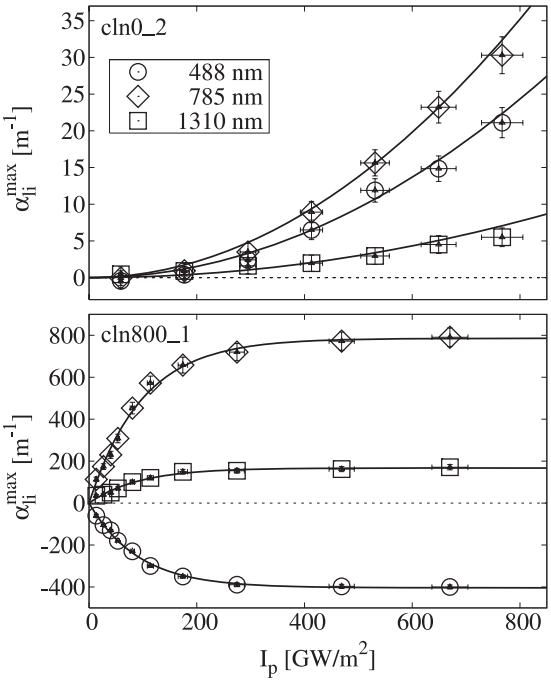

Figure 2. Amplitudes of the light-induced absorption, $\alpha_{li}^{max}(\lambda)$, versus pump intensity for the three probe wavelengths at room temperature in undoped $LiNbO_3$. Upper part: unreduced sample cln0_2; lower part: reduced sample cln800_1. For details see [20].

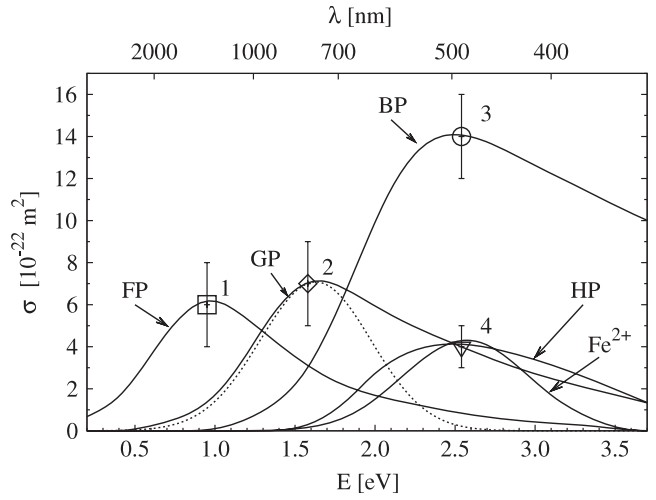

Figure 3. Absorption cross sections for small polarons as calculated in this work, and for Fe^{2+} [31]. 1: σ_{FP}(1310 nm), 2: σ_{GP}(785 nm), 3: σ_{BP}(488 nm), 4: σ_{HP}(488 nm); a more detailed examination of the absorption properties of small polarons in $LiNbO_3$ will be given in [30]. The band shapes drawn are based on data given in [7, 9, 13, 31]. The dotted line represents the theoretical polaron band shape for GP, according to [26, 27].

polarons in $LiNbO_3$ (cf [32]); further it is valid for both hole and electron polarons [7, 13, 18]. Possible reasons for this discrepancy are discussed by Schirmer ([13] and references therein) for bound small hole polarons. It will be shown in a forthcoming paper that the same arguments hold for electron single polarons and bipolarons as well [30]. Two main mechanisms are proposed for explaining qualitatively the high-frequency part of small-polaron absorption [13, 30]: (a) tunneling of the optically excited charge carrier between the possible equivalent final sites assumed to occur before the lattice relaxes; (b) transitions of the carriers to excited-state orbitals at the final sites [30]. Both effects are expected at higher photon energies and have not been considered in the standard theories for small polarons [26–29]. Additional phenomena like line broadening in disordered media will further affect the shape of the absorption bands [28]. A detailed and quantitative investigation of this rather complex subject is beyond the scope of this work.

However, since the results of our calculations depend crucially on the knowledge of the actual lineshapes of the optical absorption bands we have to use those shapes which have been derived from experimental absorption spectra, as determined in [7, 9, 13, 31]. The amplitudes of the polaron bands shown in figure 3 have been adjusted to the absorption cross sections calculated in the following. One can readily observe that the mutual spectral overlap of the polaronic absorption bands is in most cases substantial. We will consider this fact in our calculations by using the normalized dimensionless 'shape functions' $f_i(\lambda)$ such that

$$\sigma_i(\lambda) = \sigma_i(\lambda_{peak})\, f_i(\lambda), \qquad 0 \leqslant f_i(\lambda) \leqslant 1. \tag{3}$$

Table 2. Values of the lineshape function $f_i(\lambda)$ for the different kinds of photochromic centers, based on [7, 9, 13, 31]. The values are normalized to the maxima of the absorption bands.

		$f_i(\lambda)$		
Photochromic center		488 nm	785 nm	1310 nm
FP	Nb_{Nb}^{4+}	0.14 ± 0.05	0.50 ± 0.05	1.00 ± 0.05
GP	Nb_{Li}^{4+}	0.56 ± 0.05	1.00 ± 0.05	0.20 ± 0.05
BP	Nb_{Li}^{4+}:Nb_{Nb}^{4+}	0.97 ± 0.05	0.22 ± 0.05	<0.01
HP	O^-	1.00 ± 0.05	0.08 ± 0.05	<0.01
iron	Fe^{2+}	1.00 ± 0.05	0.04 ± 0.05	<0.01

A list of the values of $f_i(\lambda)$ for the relevant wavelengths and photochromic centers is given in table 2. For the sake of compactness of notation we will further write the wavelengths as superscripts in the following (e.g. $f_i(\lambda) \equiv f_i^{(\lambda)}$), also omitting the dimension of λ.

The anchor for the calculations presented in the following section is the absorption cross section of bound polarons σ_{GP}. Experimental values for this quantity have been determined using combinations of EPR and optical absorption [14, 22], and femtosecond pump–probe investigations [33]. All results point to a mean value of

$$\sigma_{GP}^{(785)} \approx (7 \pm 2) \times 10^{-22}\ \mathrm{m}^2 \tag{4}$$

for ordinary polarized light. It will, however, be seen that our calculated values for the number densities and absorption cross sections scale directly with $\sigma_{GP}^{(785)}$ ($\sigma_i \propto \sigma_{GP}^{(785)}$ and $N_{li,i} \propto (\sigma_{GP}^{(785)})^{-1}$). Thus the generality of our calculations is not affected by the specific experimental value of $\sigma_{GP}^{(785)}$.

In the following section we will first calculate the number densities of bound electron and hole polarons in unreduced $LiNbO_3$, by which means we will also determine the absorption cross section of HP. It is then possible to

use the values obtained for hole polarons to compute the relevant quantities for free polarons in $LiNbO_3$:Mg above the ODRT. Finally we are able to find the number densities and absorption cross sections of bipolarons in nominally pure, reduced $LiNbO_3$.

3. Results and discussion

In nominally pure, unreduced $LiNbO_3$, as well as in $LiNbO_3$:Mg below the ODRT, GP and HP are generated during the pump illumination via two-photon processes [20, 24]. The complexity of the decay of $\alpha_{\rm li}(t)$, namely the occurrence of multiple decay components, enforces us to account for the presence of extrinsic defects, e.g. $Fe^{2+/3+}$, as well [12, 17, 20, 24]. Although more than one extrinsic center may influence the behavior of $\alpha_{\rm li}(t)$ we will assume here only the presence of iron, since it is the most important dopant. In this case the number density of additionally generated Fe^{2+} ions in undoped $LiNbO_3$ (cln0_2) is determined to be not larger than $N_{\rm li,Fe^{2+}} \approx 2.2 \times 10^{22}$ m^{-3}, corresponding to a value for the Fe^{2+}-related light-induced absorption of $\alpha_{\rm li}^{\rm max}(Fe^{2+}) \approx 10$ m^{-1} at $\lambda = 488$ nm [20, 31].

According to [12, 20] the population of residual Fe centers ($Fe^{3+} \rightarrow Fe^{2+}$) occurs only via GP. Depending on the actual iron concentration and pump intensity, this process takes at least several microseconds [12, 20]. Therefore we assume that the initial number density of light-induced hole polarons—observed directly after the pump pulse—equals that of GP. Using equations (1)–(3), we may calculate the absorption cross sections and number densities of HP:

$$\sigma_{\rm HP}^{(488)} = \sigma_{\rm GP}^{(785)} \frac{\alpha_{\rm li}^{\rm max}(785)\, f_{\rm GP}^{(488)} - \alpha_{\rm li}^{\rm max}(488)\, f_{\rm GP}^{(785)}}{\alpha_{\rm li}^{\rm max}(488)\, f_{\rm HP}^{(785)} - \alpha_{\rm li}^{\rm max}(785)\, f_{\rm HP}^{(488)}} \approx 4.2 \times 10^{-22}\ {\rm m}^2, \tag{5}$$

and

$$N_{\rm li,HP} = \frac{1}{\sigma_{\rm GP}^{(785)}} \frac{\alpha_{\rm li}^{\rm max}(785)\, f_{\rm HP}^{(488)} - \alpha_{\rm li}^{\rm max}(488)\, f_{\rm HP}^{(785)}}{f_{\rm GP}^{(785)} f_{\rm HP}^{(488)} - f_{\rm GP}^{(488)} f_{\rm HP}^{(785)}} \approx 1.2 \times 10^{23}\ {\rm m}^{-3}. \tag{6}$$

In this calculation the values obtained for the Mg-doped sample cln149912.1 were used. Using the values for cln0_2, one finds $\sigma_{\rm HP}^{(488)} \approx 1.0 \times 10^{-22}$ m^2 and $N_{\rm li,HP} = N_{\rm li,GP} \approx 4.2 \times 10^{22}$ m^{-3}. We will use the former values for two reasons: first, the signal-to-noise ratio is substantially larger than in the latter case; second, the absorption bands obtained (see [24]) correspond closely to those found in previous studies [11, 34]. A possible reason for the deviating behavior of sample cln0_2 may be incomplete oxidation, which leads to smaller amplitudes $\alpha_{\rm li}^{\rm max}$ in the blue spectral range [20].

We can use the absorption cross section of HP to examine the light-induced absorption in $LiNbO_3$:Mg above the ODRT (cln140704.1). Like for nominally pure, unreduced samples, hole polarons and free polarons are initially generated upon illumination [24, 25], while Fe^{2+} is populated subsequently. Using equations (5) and (6) in their respective forms, one finds for the light-induced hole polaron density $N_{\rm li,HP} \approx 3.0 \times 10^{23}$ m^{-3}. Consequently for free polarons the following values are obtained: $N_{\rm li,FP} = N_{\rm li,HP}$ and $\sigma_{\rm FP}^{(1310)} \approx 5.5 \times 10^{-22}$ m^2. Provided that iron is the observed extrinsic center, after the recombination of FP (taking several microseconds), the residual electrons are trapped as Fe^{2+}, so $N_{\rm li,Fe^{2+}} = N_{\rm li,HP,residual}$. Hence, the full iron-related light-induced absorption is estimated to be less than $\alpha_{\rm li}^{\rm max}(Fe^{2+}) = 30$ m^{-1}, yielding $N_{\rm li,Fe^{2+}} \leqslant 6.7 \times 10^{22}$ m^{-3} (that is $[Fe_{\rm li}^{2+}] \leqslant 3.4$ ppm), with the relevant absorption cross section $\sigma_{Fe^{2+}}(488\ {\rm nm}) \approx 4.5 \times 10^{-22}$ m^2 [31].

In order to determine the number density and absorption cross section of bipolarons, we investigate the data obtained for the reduced sample cln800_1, for which the influence of residual Fe is negligible [20]. At the pump intensities used here, a saturation of the light-induced absorption changes at $\lambda = 488$ and 785 nm is observed (see figure 2) [15, 20]. It was assumed that in this case no free polarons, but only bound polarons are created upon optical dissociation of reduction-induced bipolarons [19, 20]. The law of charge conservation then leads to the relation

$$N_{\rm li,GP} = -2N_{\rm li,BP}. \tag{7}$$

Combining this with (1) and (2) we find relations for σ_i and N_i which slightly differ from equations (5) and (6), namely

$$\sigma_{\rm BP}^{(488)} = -2\,\sigma_{\rm GP}^{(785)} \frac{\alpha_{\rm li}^{\rm max}(785)\, f_{\rm GP}^{(488)} - \alpha_{\rm li}^{\rm max}(488)\, f_{\rm GP}^{(785)}}{\alpha_{\rm li}^{\rm max}(488)\, f_{\rm BP}^{(785)} - \alpha_{\rm li}^{\rm max}(785)\, f_{\rm BP}^{(488)}} \approx 13.8 \times 10^{-22}\ {\rm m}^2, \tag{8}$$

and

$$N_{\rm li,BP} = -\frac{1}{2\,\sigma_{\rm GP}^{(785)}} \frac{\alpha_{\rm li}^{\rm max}(785)\, f_{\rm BP}^{(488)} - \alpha_{\rm li}^{\rm max}(488)\, f_{\rm BP}^{(785)}}{f_{\rm GP}^{(785)} f_{\rm BP}^{(488)} - f_{\rm GP}^{(488)} f_{\rm BP}^{(785)}} \approx -7.2 \times 10^{23}\ {\rm m}^{-3}. \tag{9}$$

Hence, the number density of light-induced bound polarons is $N_{\rm li,GP} \approx 1.4 \times 10^{24}$ m^{-3}. These values may be compared to those reported by Dutt *et al* ($N_{\rm BP} \approx 1 \times 10^{24}$ m^{-3}, $\sigma_{\rm BP}^{(\rm conv.)}(488\ {\rm nm}) \approx 3 \times 10^{-22}$ m^2) [35]. The discrepancy for the values of $\sigma_{\rm BP}$ could be due to the fact that in [35] a so-called 'conversion cross section' is determined, which already incorporates the quantum efficiency for the dissociation of bipolarons, and which is hence significantly smaller than our value for the sole absorption without dissociation.

It is further possible to determine the steady-state concentrations of BP and GP at room temperature: a careful examination of the steady-state absorption $\alpha(\lambda)$ of the sample cln800_1 leads to absorption values $\alpha(488\ {\rm nm}) = 1040$ m^{-1} and $\alpha(785\ {\rm nm}) = 460$ m^{-1} without illumination at room temperature [20]. From these data we calculate the steady-state number density of bipolarons and bound polarons at room temperature to be

$$N_{\rm BP}^{\rm RT} = -\frac{1}{\sigma_{\rm BP}^{(488)}} \frac{\alpha(785)\, f_{\rm GP}^{(488)} - \alpha(488)\, f_{\rm GP}^{(785)}}{f_{\rm GP}^{(785)} f_{\rm BP}^{(488)} - f_{\rm GP}^{(488)} f_{\rm BP}^{(785)}} \approx 6.7 \times 10^{23}\ {\rm m}^{-3} \tag{10}$$

that is, $|N_{\rm BP}^{\rm RT}| \approx |N_{\rm li,BP}|$, and

$$N_{\rm GP}^{\rm RT} = -\frac{1}{\sigma_{\rm GP}^{(785)}} \cdot \frac{\alpha(785)\, f_{\rm BP}^{(488)} - \alpha(488)\, f_{\rm BP}^{(785)}}{f_{\rm GP}^{(785)} f_{\rm BP}^{(488)} - f_{\rm GP}^{(488)} f_{\rm BP}^{(785)}} \approx 3.7 \times 10^{23}\ {\rm m}^{-3}, \tag{11}$$

Table 3. Estimated number densities and absorption cross sections for the different kinds of photochromic centers. For bipolarons the number density in the dark is given (see equation (10)).

Photochromic center		N (10^{22} m^{-3})	N/N_{sites}	σ (10^{-22} m^2)	λ (nm)	Sample	Ref.
FP	Nb_{Nb}^{4+}	30 ± 5	1.5×10^{-5}	6 ± 2	1310	cln140704.1	
GP	Nb_{Li}^{4+}	12 ± 3	6.0×10^{-4}	7 ± 2	785	cln149912.1	[14, 22, 23]
BP	Nb_{Li}^{4+}:Nb_{Nb}^{4+}	70 ± 8	3.5×10^{-3}	14 ± 2	488	cln800_1	
HP	O^-	30 ± 5	3.8×10^{-4}	4 ± 1	488	cln140704.1	
Iron	Fe^{2+}	2 ± 1	—	4.5 ± 0.8	488	cln0_2	[20, 31]

yielding a total concentration of reduction-induced electrons of

$$N_{\text{el}} = 2N_{\text{BP}} + N_{\text{GP}} \approx 1.7 \times 10^{24}\ \text{m}^{-3}. \qquad (12)$$

A number of conclusions may be drawn from this finding:

(i) The bipolaron concentration at room temperature is about 3.5×10^{-3} of the possible bipolaron sites.
(ii) At room temperature, a substantial amount (≈20%) of the reduction-induced electrons are present as bound polarons (cf Koppitz *et al* [9]).
(iii) The total amount of excess electrons implies a reduction condition where about 1.5×10^{-5} of the O^{2-} ions are removed during the reduction process, assuming an oxygen concentration of $N_{O^{2-}} \approx 6 \times 10^{28}$ m^{-3}. Hence, we are dealing with 'low degrees of reduction' (cf [10]). Note that this does not imply the presence of oxygen vacancies. For detailed discussions see [10, 18, 30, 36].
(iv) The concentration of light-induced bound polarons has reached a saturation for the pump intensities used in our setup, accompanied by a complete dissociation of reduction-induced bipolarons. Equivalent results were obtained by Jermann *et al* for more strongly reduced samples, where the appropriate pump beam intensity for saturation has been lower than in our case [15].
(v) The absorption cross section of bipolarons is nearly twice as large as for bound small polarons.

Summarizing our investigations, it is remarkable that the values of σ_i at the maxima of the specific absorption bands are apparently very similar for all kinds of single small polarons in $LiNbO_3$. They are furthermore comparable to that of Fe^{2+}, which is the most important extrinsic impurity center [31]. The absorption cross section of bipolarons is roughly twice as large as that for single small polarons. An overview of the calculated parameters is given in table 3 and further illustrated in figure 3. The ratio N/N_{sites} is calculated using for FP the number density of regular Nb sites ($N_{\text{Nb}_{\text{Nb}}} \approx 2 \times 10^{28}$ m^{-3}), while for GP and BP the density of antisite defects is relevant ($N_{\text{Nb}_{\text{Li}}} \approx 2 \times 10^{26}$ m^{-3}; see above). The number density of possible HP sites equals that of the Li vacancies ($N_{\text{V}_{\text{Li}}} \approx 8 \times 10^{26}$ m^{-3}) [10]. Please note that the values in table 3 are rounded according to the experimental accuracy. It has to be mentioned further that the numbers calculated here depend on the actual model implied in [12, 20]. Alternative models taking into account, e.g., additional excitation paths, may result in slightly different values for N_i and σ_i. In any case one finds that the number density of both reduction-induced and optically generated small polarons is less than 1% of the possible polaron sites in the $LiNbO_3$ samples investigated.

The method presented in this work may be applied to other materials as well—for instance in combination with EPR analyses [37]—to determine number densities and absorption cross sections of intrinsic and extrinsic photochromic centers. Within this area, an extension to borate crystals (LiB_3O_5, β-BaB_2O_4, etc) would be of special interest due to their common application in high-power laser systems [1, 2, 38].

Acknowledgments

Financial support by the Deutsche Forschungsgemeinschaft (Fund Nos IM 37/5-1, TFB 13-04, and GRK 695) and the Hungarian Science and Research Fund (Grants K60086 and T047265) is gratefully acknowledged.

References

[1] Furukawa Y, Markgraf S A, Sato M, Yoshida H, Sasaki T, Fujita H and Yamanaka T 1994 *Appl. Phys. Lett.* **65** 1480
[2] Scripsick M P, Fang X H, Edwards G H, Halliburton L E and Tyminski J K 1993 *J. Appl. Phys.* **73** 1114
[3] Setzler S D, Stevens K T, Fernelius N C, Scripsick M P, Edwards G J and Halliburton L E 2003 *J. Phys.: Condens. Matter* **15** 3969–84
[4] Wevering S, Imbrock J and Krätzig E 2001 *J. Opt. Soc. Am.* B **18** 472–8
[5] Mabuchi H, Polzik E S and Kimble H J 1994 *J. Opt. Soc. Am.* B **11** 2023–9
[6] Furukawa Y, Kitamura K, Alexandrowski A, Route R K, Fejer M M and Foulon G 2001 *Appl. Phys. Lett.* **78** 1970–2
[7] Faust B, Müller H and Schirmer O F 1994 *Ferroelectrics* **153** 297–302
[8] Schirmer O F, Juppe S and Koppitz J 1987 *Cryst. Latt. Defects. Amorph. Mater.* **16** 353–7
[9] Koppitz J, Schirmer O F and Kuznetsov A I 1987 *Europhys. Lett.* **4** 1055–9
[10] Smyth D M 1983 *Ferroelectrics* **50** 93–102
[11] Schirmer O F and von der Linde D 1978 *Appl. Phys. Lett.* **33** 35–8
[12] Herth P, Granzow T, Schaniel D, Woike Th, Imlau M and Krätzig E 2005 *Phys. Rev. Lett.* **95** 067404
[13] Schirmer O F 2006 *J. Phys.: Condens. Matter* **18** R667–704
[14] Sweeney K L and Halliburton L E 1983 *Appl. Phys. Lett.* **43** 336–8
[15] Jermann F, Simon M, Böwer R, Krätzig E and Schirmer O F 1995 *Ferroelectrics* **165** 319–27
[16] Berben D, Buse K, Wevering S, Herth P, Imlau M and Woike Th 2000 *J. Appl. Phys.* **87** 1034–41
[17] Herth P, Schaniel D, Woike Th, Granzow T, Imlau M and Krätzig E 2005 *Phys. Rev.* B **71** 125128
[18] Schirmer O F, Thiemann O and Wöhlecke M 1991 *J. Phys. Chem. Solids* **52** 185–200
[19] Merschjann C, Berben D, Imlau M and Wöhlecke M 2006 *Phys. Rev. Lett.* **96** 186404

[20] Merschjann C, Schoke B and Imlau M 2007 *Phys. Rev.* B **76** 085114
[21] Merschjann C, Schoke B, Conradi D and Imlau M 2007 *Controlling Light with Light: Photorefractive Effects, Photosensitivity, Fiber Gratings, Photonic Materials and More* CD-ROM, ISBN 1-55752-848-9:SuB5
[22] Jermann F and Otten J 1993 *J. Opt. Soc. Am.* B **10** 2085–92
[23] Beyer O, Maxein D, Buse K, Sturman B, Hsieh H T and Psaltis D 2005 *Phys. Rev.* E **71** 056603
[24] Conradi D, Merschjann C, Imlau M, Corradi G and Polgár K 2008 *Phys. Status Solidi (RRL)* **2** 284–6
[25] Conradi D, Merschjann C, Schoke B and Imlau M 2007 *Controlling Light with Light: Photorefractive Effects, Photosensitivity, Fiber Gratings, Photonic Materials and More* CD-ROM, ISBN 1-55752-848-9:MB3
[26] Reik H G and Heese D 1967 *J. Phys. Chem. Solids* **28** 581–96
[27] Emin D 1993 *Phys. Rev.* B **48** 13691–702
[28] Alexandrov A S and Bratkovsky A M 1999 *J. Phys.: Condens. Matter* **11** L531–9
[29] Loos J, Hohenadler M, Alvermann A and Fehske H 2007 *J. Phys.: Condens. Matter* **19** 236233
[30] Schirmer O F, Imlau M, Merschjann C and Schoke B 2008 *J. Phys.: Condens. Matter* submitted
[31] Kurz H, Krätzig E, Keune W, Engelmann H, Gonser U, Dischler B and Räuber A 1977 *Appl. Phys.* **12** 355–68
[32] Bi X X and Eklund P C 1993 *Phys. Rev. Lett.* **70** 2625–8
[33] Beyer O, Maxein D, Woike Th and Buse K 2006 *Appl. Phys.* B **83** 527–30
[34] Arizmendi L, Cabrera J M and Agulló-López F 1984 *J. Phys. C: Solid State Phys.* **17** 515–29
[35] Dutt D A, Feigl F J and DeLeo G G 1990 *J. Phys. Chem. Solids* **51** 407–15
[36] Donnerberg H J, Tomlinsson S M and Catlow C R A 1991 *J. Phys. Chem. Solids* **52** 201–10
[37] Meyer M, Schirmer O F and Pankrath R 2004 *Appl. Phys.* B **79** 395–408
[38] Sasaki T, Mori Y, Yoshimura M, Yap Y K and Kamimura T 2000 *Mater. Sci. Eng.* R **30** 1–54